

# ORGANOMETALLICS

Volume 8, Number 6, June 1989

© Copyright 1989  
American Chemical Society

## Probing the Chemistry of Organomanganese Complexes: Correlation of Chemical Reactivity, Manganese-55 NMR Chemical Shifts, and Molecular Orbital Studies of Organomanganese Complexes. Aromaticity of an Organomanganese Complex

Phillip DeShong,\* Greg A. Slough,<sup>†</sup> Daniel R. Sidler, and Philip J. Rybczynski

Department of Chemistry and Biochemistry, University of Maryland, College Park, Maryland 20742

Wolfgang von Philipsborn\* and Roland W. Kunz

Organisch-chemisches Institut, University of Zürich, Winterthurerstrasse 190, CH-8057 Zürich, Switzerland

Bruce E. Bursten\* and Thomas W. Clayton, Jr.

Department of Chemistry, The Ohio State University, Columbus, Ohio 43210

Received April 6, 1988

Manganese-55 nuclear magnetic resonance spectroscopy has been employed to probe the structure of various organomanganese(I) complexes. The chemical shift of the metal is indicative of the electron distribution in the complexes and can be correlated with the chemical reactivity of the respective complexes. Molecular orbital calculations were performed upon metallacyclic complexes of manganese in an investigation of bonding, electron distribution, and reactivity. The role of a carbonyl oxygen heteroatom in stabilization of these complexes was examined in order to explain experimental evidence for aromatic character observed for an unsaturated manganacycle.

### Introduction

We have recently demonstrated that alkylmanganese pentacarbonyl complexes (1) react with either alkenes or alkynes to afford novel organomanganese complexes (manganacycles) 2 or 3, respectively. Manganacycles 2 and 3 arise from insertion of carbon monoxide and the unsaturated component in a sequential fashion as depicted in Scheme I, and the resulting adducts are versatile intermediates in the synthesis of organic substances.<sup>1</sup>

During subsequent studies with complexes 1-3, significant differences in the reactivity of the respective manganese complexes were noted. For example, complexes 1-3 are formally Mn(I) in oxidation state, yet only alkylmanganese pentacarbonyl complexes (1) underwent migratory insertion of carbon monoxide to provide acylmanganese complexes.<sup>2</sup> The "saturated" (2) and "unsaturated" manganacycles (3), on the other hand, displayed no tendency to insert carbon monoxide even under stringent conditions.<sup>1</sup>

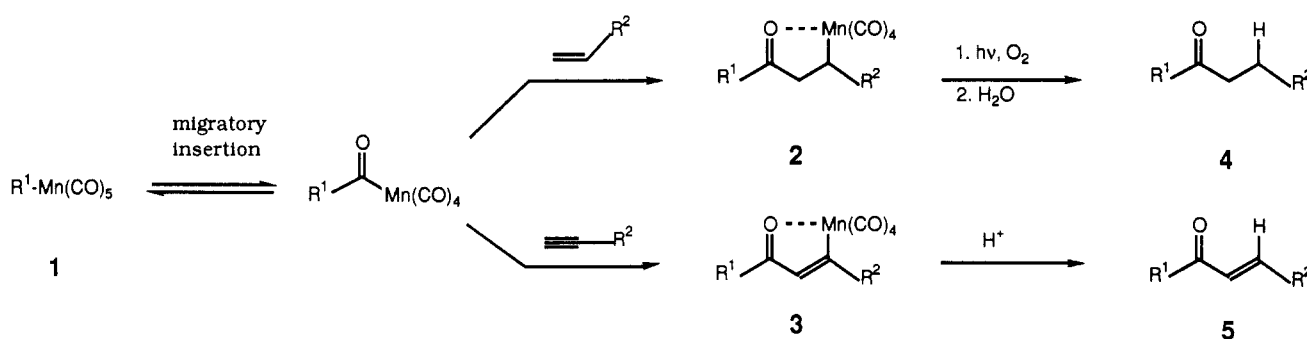
A second indication of the reactivity differences associated with these organomanganese complexes was observed in the demetalation reactions of manganacycles 2 and 3, respectively. Photodemetalation of 2 ( $R^2 = COOMe$ )

(1) (a) DeShong, P.; Slough, G. A. *Organometallics* 1984, 3, 636. (b) DeShong, P.; Slough, G. A.; Elango, V.; Trainor, G. L. *J. Am. Chem. Soc.* 1985, 107, 7788. (c) DeShong, P.; Slough, G. A.; Rheingold, A. L. *Tetrahedron Lett.* 1987, 28, 2229. (d) DeShong, P.; Slough, G. A.; Sidler, D. R. *Ibid.* 1987, 28, 2233. (e) DeShong, P.; Slough, G. A.; Elango, V. *Carbohydr. Res.* 1987, 171, 342. (f) DeShong, P.; Sidler, D. R.; Rybczynski, P. J.; Slough, G. A.; Rheingold, A. L. *J. Am. Chem. Soc.* 1988, 110, 2575.

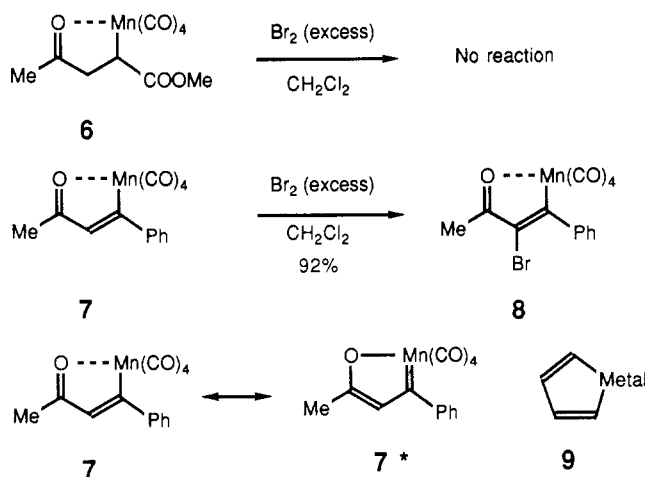
(2) For leading references to discussion of migratory insertion processes see: (a) Collman, J. P.; Hegedus, L. S.; Norton, J. R.; Finke, R. G. *Principles and Applications of Organotransition Metal Chemistry*; University Science Books: Mill Valley, CA, 1987; pp 356-376. Kuhlman, E. J.; Alexander, J. J. *Coord. Chem. Rev.* 1980, 33, 195-225. Wojcicki, A. *Adv. Organomet. Chem.* 1973, 11, 88. Davies, S. G. *Organotransition Metal Chemistry: Applications to Organic Synthesis*; Pergamon: Oxford, 1983; pp 348-392. Wender, I.; Pino, P. *Organic Synthesis via Metal Carbonyls*; Interscience: New York 1977; Vols. 1 and 2. Kahn, M. M. T.; Martell, A. E. *Homogenous Catalysis by Metal Complexes*; Academic Press: New York, 1974, Vol. 1. (b) Noack, K.; Calderazzo, F. *J. Am. Chem. Soc.* 1967, 89, 101. Calderazzo, F. *Angew. Chem., Int. Ed. Engl.* 1977, 16, 299. (c) Casey, C. P.; Bunnell, C. A.; Calbrese, J. C. *J. Am. Chem. Soc.* 1976, 98, 1166 and references cited therein. (d) Flood, T. C.; Jensen, J. E.; Statler, J. A. *J. Am. Chem. Soc.* 1981, 103, 4410. Flood, T. C. *Top. Stereochem.* 1980, 12, 37.

<sup>†</sup>Current address: Department of Chemistry, College of Wooster, Wooster, OH 44691.

Scheme I



Scheme II



or  $\text{SO}_2\text{Ph}$ ) proceeded readily to furnish ketone 4. In contrast, photolysis of complex 3 failed to provide demetalated product; instead, removal of manganese from 3 was effected with anhydrous acid (Scheme I).<sup>1</sup>

More intriguing still, it was observed that "saturated" manganacycle 6 could be recovered unchanged upon treatment with excess bromine in methylene chloride, while the "unsaturated" analogue 7 furnished brominated complex 8 under identical halogenation conditions.<sup>3</sup> The stability of the carbon-metal bond in manganacycles 2 and 3 toward electrophilic reagents is in stark contrast to alkylmanganese pentacarbonyl complexes (1) which are known to react under these conditions to yield the corresponding alkyl bromide and bromomanganese pentacarbonyl. Replacement of the C-2 hydrogen of 7 with a bromine atom is analogous to a classical electrophilic aromatic substitution process. The exceptional stability of the carbon-metal bond in this system suggested that "unsaturated" manganacycles possess unusual bonding characteristics, and we propose that complex 3 is aromatic (vide infra). A resonance form of  $d^6$  complex 7 in which the manganacycle ring is represented as a metallafuran derivative is 7\* and thus would be related to the metallapentadiene complexes 9.<sup>3</sup>

### Manganese-55 Nuclear Magnetic Resonance Spectroscopy

The differences observed in the reactivity of complexes 1, 2, and 3 summarized above indicated that the electronic

Table I.  $^{55}\text{Mn}$  NMR Chemical Shift Data

Mn complex	chem shift, $\delta$	$w_{1/2}$ , kHz
Type 1 Complexes		
$\text{MeMn}(\text{CO})_5$	-2265 <sup>a</sup>	2.7
$\text{Mn}(\text{CO})_5$	-2095	2.5
$\text{PhCH}_2\text{Mn}(\text{CO})_4(\text{PBu}_3)$	-2060	13.5
$\text{PhCH}_2\text{Mn}(\text{CO})_5$	-2020 <sup>b</sup>	4.2
$\text{PhMn}(\text{CO})_5$	-2000	6.5
$\text{CH}_3\text{C}(\text{O})\text{Mn}(\text{CO})_4(\text{PBu}_3)$	-1978	16.0
$\text{PhCH}_2\text{C}(\text{O})\text{Mn}(\text{CO})_4(\text{PBu}_3)$	-1933	21.5
$\text{PhCH}_2\text{Mn}(\text{CO})_4(\text{PPh}_3)$ (10)	-1819 <sup>b,c</sup>	0.3
Type 2 Complexes: "Saturated" Manganacycles		
$\text{R}^1\text{-Mn}(\text{CO})_4$	-689	13.4
$\text{R}^1\text{-Mn}(\text{CO})_4$	-670	27.0
$\text{R}^1 = \text{Me}, \text{PhCH}_2$		
Type 3 Complexes: "Unsaturated" Manganacycles		
$\text{R}^3\text{-Mn}(\text{CO})_4$	-821	18.0
$\text{R}^3\text{-Mn}(\text{CO})_4$	-807	26.0
$\text{R}^3 = \text{Me}, \text{PhCH}_2$		

<sup>a</sup> In THF, see ref 4. <sup>b</sup> In  $\text{CDCl}_3$ , 301 K. <sup>c</sup>  $J(^{55}\text{Mn}, ^{31}\text{P}) = 267$  Hz.

characteristics of the ligands had a strong influence upon the chemistry associated with the respective complexes. This aspect of the chemistry of manganese(I) complexes was subsequently probed employing  $^{55}\text{Mn}$  nuclear magnetic resonance spectroscopy<sup>4,5</sup> and molecular orbital calculations to ascertain the unique bonding and electronic characteristics of manganacycles 2 and 3 which distinguish these complexes from the parent alkylmanganese pentacarbonyl systems (1).

Chemical shift data for a series of Mn(I) complexes are compiled in Table I. The chemical shift data fall into three broad categories depending upon the structure of the organomanganese complex. Alkylmanganese pentacarbonyl (1) and related complexes such as benzylmanganese tetracarbonyl triphenylphosphine (10) displayed chemical shifts in the range of  $\delta$  -1800 to -2300.<sup>5</sup> The  $^{55}\text{Mn}$  chemical shifts are most readily understood in terms of the shielding of the manganese nucleus relative to the standard. The shielding of the nucleus is described as the sum of both diamagnetic and paramagnetic contributions, although for a given polyelectronic atom the diamagnetic shielding is primarily related to the core electron density and can be regarded as nearly constant in  $d^6$  systems.<sup>6a</sup> In fact, in an ab initio study for a series

(3) (a) For a general discussion of metallapentadiene systems and their role in acetylene trimerization see; Collman, J. P.; Hegedus, L. S.; Norton, J. R.; Finke, R. G. *Principles and Applications of Organotransition Metal Chemistry*; University Science Books: Mill Valley, CA; 1987; pp 509-512 and references cited therein. (b) For a discussion of the aromaticity of metallacyclopentadiene complexes from a theoretical perspective see: Thorn, D. L.; Hoffmann, R. *Nouv. J. Chim.* 1979, 3, 39 and references cited therein.

(4) (a) Rehder, D. *Magn. Reson. Rev.* 1984, 9, 164. (b) Philipsborn, W. v. *Pure Appl. Chem.* 1986, 58, 513.

(5) For additional examples of  $^{55}\text{Mn}$  chemical shift data see ref 4a and 8. See also: Onaka, S.; Sugawara, T.; Kawada, Y.; Yokoyama, Y.; Iwamura, H. *Bull. Chem. Soc. Jpn.* 1986, 59, 3079. Onaka, S.; Miyamoto, T.; Sasaki, Y. *Bull. Chem. Soc. Jpn.* 1971, 44, 1851. Miles, W. J., Jr.; Garret, B. B.; Clark, R. J. *Inorg. Chem.* 1969, 8, 2817.

of related manganese complexes, Nakatsuji demonstrated that 3d-electron contributions to the paramagnetic shielding dominate the chemical shift equation and determine the chemical shift of the metal nucleus.<sup>6b</sup> Paramagnetic shielding results from mixing of the ground state with various magnetically sensitive electronic excited states by the magnetic field.<sup>6c</sup> An increase in the paramagnetic contribution deshields the nucleus and subsequently results in a chemical shift at higher frequency. Calderazzo et al. demonstrated that this paramagnetic shift to higher frequency increases as the covalent strength of the Mn-X bond decreases for a series of manganese pentacarbonyl complexes.<sup>6d</sup> Nakatsuji et al. correlated the increasing paramagnetic shift contribution with increasing hardness of the ligand (a  $\sigma$ -effect) and with increasing ligand  $\pi$ -donor ability.<sup>6b</sup> The variation in chemical shift within the type 1 complexes seen in Table I is thus generally consistent with the results of Nakatsuji wherein the replacement of a  $\pi$ -acidic ligand such as carbon monoxide by a  $\sigma$ -donating phosphine ligand results in a chemical shift at lower field (vide infra).

The major anomaly in the data summarized within Table I arises from comparison of the chemical shift of tributyl- and triphenylphosphine analogues with the parent pentacarbonyl system. For example, benzylmanganese pentacarbonyl shows a metal chemical shift at  $\delta$  -2020, and, based on the hypothesis of Nakatsuji, we expected that the corresponding phosphine analogues would show chemical shifts at higher frequency. In fact, replacement of CO by triphenylphosphine resulted in a ca. 200 ppm paramagnetic (high-frequency) shift, thus illustrating the weaker  $\pi$ -acceptor property of this phosphine ligand. However, the corresponding tributyl analogue displays a  $\delta$  -2060 signal for the metal, a shift to lower frequency than the parent system. We attribute this anomalous behavior to a subtle interplay of  $\sigma$ -effects in the respective phosphine complexes since both tributyl- and triphenylphosphine are much weaker  $\pi$ -acceptor ligands than carbon monoxide. For steric and electronic reasons, triphenylphosphine is a weaker  $\sigma$ -donor than the corresponding butyl derivative, and consequently, tributylphosphine is a better overall donor. Therefore, the slightly increased shielding observed upon substitution of CO by tributylphosphine can be attributed to a large increase in  $\sigma$ -donor ability, thus overcompensating for the loss of  $\pi$ -acceptor character. The validity of this relationship of chemical shifts to ligand  $\sigma$ -bonding effects is speculative within such a small sampling of chemical shift data, and it will be necessary to consider a larger data set of experimental measurements before we can be secure with this hypothesis.

As anticipated from the reactivity profile, manganacycles 2 and 3 exhibit markedly different chemical shifts for the metal than displayed in complexes of type 1. Manganacycles appear in the range of  $\delta$  -670 to -820, ~1400 ppm downfield of the related alkylmanganese pentacarbonyl complexes. This significant change in the chemical shift of the metal is remarkable since replacement of carbon monoxide by phosphine in type 1 complexes did not result in substantial alteration in metal chemical shifts (vide supra). The large changes in chemical shifts associated with the manganacycles suggest that even though manganese is formally in the +1 oxidation state in type 2 and

type 3 manganacycles, the electron density distribution in the manganacycles is dramatically altered upon the transformation of 1 to either manganacycle. The deshielding of the metal in manganacycles 2 and 3 reflects a significant change of the electron density and/or the anisotropy of its distribution on the metal, implying a strong perturbation of the manganese by the ketone carbonyl.<sup>6e</sup> As discussed above, Nakatsuji has shown that the electronic distribution in the metal d orbital configuration plays a central role in the chemical shift of the metal and that ligand substitution influences the distribution of d orbitals. The low symmetry of the manganacycles, however, does not permit further qualitative discussion in terms of a  $\sigma, \pi$ -separation. Ligands also alter the electronic charge on the metal which results in chemical shift changes.<sup>6b</sup> The nature of this strong perturbation of the metal by the ketonic oxygen atom was investigated in the molecular orbital study discussed in due course. Moreover, the net electron donation to the metal is calculated to be 0.06 e larger for the unsaturated manganacycles as compared to the saturated complexes. This may contribute to the chemical shift difference of about 140 ppm between type 2 and type 3 complexes.

There is a correlation between the trends observed for the chemical shift data and the reactivity of complexes 1-3. Alkylmanganese pentacarbonyl complexes (1) that show a highly shielded <sup>55</sup>Mn nucleus undergo facile migratory insertion of carbon monoxide to afford acylmanganese complexes. The susceptibility of metal complexes to undergo migratory insertion is known to be extremely sensitive to the electron density on the metal, with electron-rich alkyl groups being the most reactive.<sup>7</sup>

Application of <sup>55</sup>Mn nuclear magnetic resonance spectroscopy to the study of manganese complexes 1-3 provides insight into the effects of ligands at the metal center by allowing correlation of data from chemical reactivity studies with chemical shift parameters. For example, manganese(I) complexes that have more negative  $\delta$ (<sup>55</sup>Mn) than -1900 readily undergo migratory insertion. By contrast, complexes with chemical shifts below this value are resistant to subsequent insertion of carbon monoxide. A similar quantitative study has been reported in the correlation of homogeneous catalytic activity with <sup>59</sup>Co NMR shielding of RCpCo(COD) complexes.<sup>8</sup>

A second trend emerges from the data reported in Table I. For the three type 1 complexes listed, the chemical shift of the metal correlates with the relative rates of migratory insertion for these complexes. Pruett et al.<sup>7a</sup> have previously reported that methylmanganese pentacarbonyl underwent acyl formation approximately 10<sup>3</sup> times faster than the corresponding benzyl complex. Similarly, complex 10 (see Table I) was resistant to migratory insertion under conditions in which the benzyl complex furnished the acyl complex. Whether this trend in reactivity will be borne out by subsequent studies relating to migratory insertion will be determined in due course.

### Fenske-Hall Calculations

In the preceding section, results from chemical reactivity and <sup>55</sup>Mn NMR studies were described which indicated

(6) (a) Rehder, D.; Bechtholdt, H.-C.; Kecec, A.; Schmidt, H.; Siewing, M. Z. *Naturforsch.*, B, 1982, 37B, 631. (b) Kanda, K.; Nakatsuji, H.; Yonezawa, T. *J. Am. Chem. Soc.* 1984, 106, 5888. (c) Griffith, J. S.; Orgel, L. E. *Trans. Faraday Soc.* 1957, 53, 601. (d) Calderazzo, F.; Lucken, E. A. C.; Williams, D. F. *J. Chem. Soc. A* 1967, 154. (e) Jameson, C. J.; Gutowsky, H. S. *J. Chem. Phys.* 1964, 40, 1714.

(7) (a) Cawse, J. N.; Fiato, R. A.; Pruett, R. L. *J. Organomet. Chem.* 1979, 172, 405. (b) Cotton, J. D.; Crisp, G. T.; Daly, V. A. *Inorg. Chim. Acta* 1981, 47, 165. (c) Berke, H.; Hoffman, R. *J. Am. Chem. Soc.* 1978, 100, 7224. (d) Axe, F. U.; Marynick, D. S. *J. Am. Chem. Soc.* 1988, 110, 3728 and references cited therein.

(8) Bönemann, H.; Brijoux, W.; Brinkmann, R.; Meurers, W.; Mynoth, R.; Philipsborn, W. v.; Ego, T. *J. Organomet. Chem.* 1984, 272, 231. Bönemann, H. *Angew. Chem., Int. Ed. Engl.* 1985, 24, 248. For a related study of <sup>95</sup>Mo complexes see: Green, J. C.; Grieves, R. A.; Mason, J. *J. Chem. Soc., Dalton Trans.* 1986, 1313.

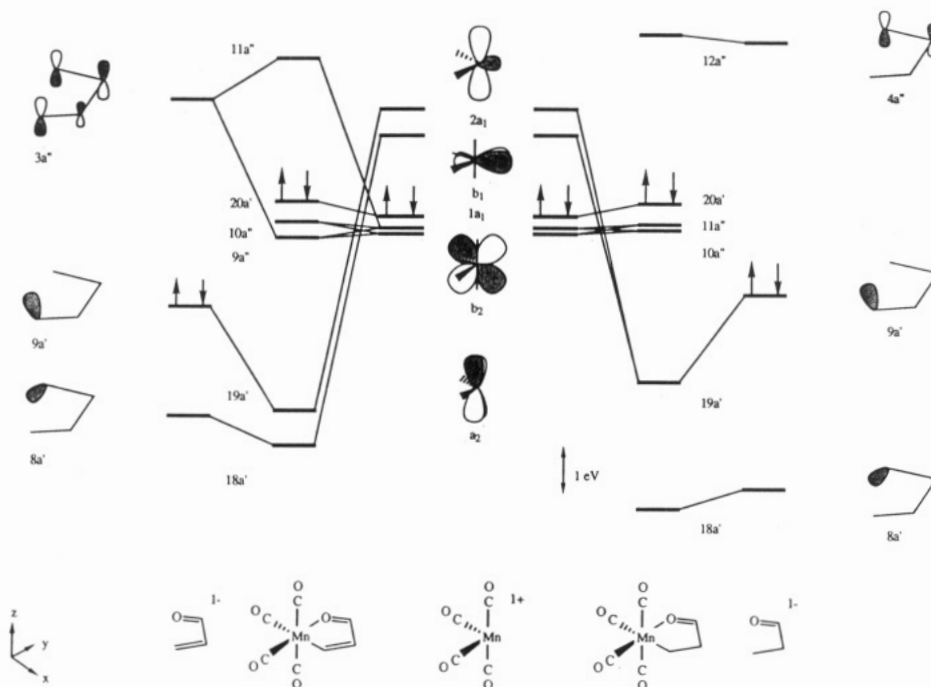
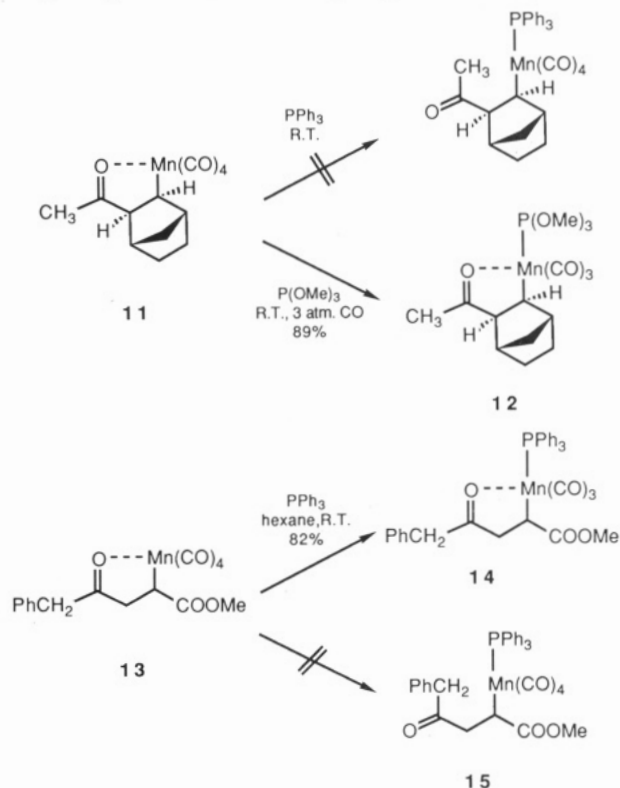


**Figure 1.** Molecular orbital diagram for manganacycles **2** and **3** showing the interaction of the  $\text{Mn}(\text{CO})_4^+$  fragment with the  $\text{C}_3\text{H}_5\text{O}^-$  and  $\text{C}_3\text{H}_3\text{O}^-$  fragments.

that the electronic environment about manganese in complexes **1**–**3** was different. In each family of complexes, manganese is formally in the +1 oxidation state; even so, each complex underwent chemical transformations unique to that family.<sup>1</sup> To gain additional insight into the bonding patterns and electron distribution properties of these complexes and to determine which factor(s) was (were) responsible for the observed differences in reactivity, a computational study of type **2** and type **3** manganacycles was undertaken.

We have performed Fenske–Hall molecular orbital calculations<sup>9</sup> on model systems of **2** and **3** where both  $\text{R}_1$  and  $\text{R}_2 = \text{H}$ ,<sup>10</sup> which lead to the orbital interaction diagrams shown in Figure 1. Both manganese complexes **2** and **3** possess pseudooctahedral geometry and can be understood in terms of the well-known orbitals of the  $\text{Mn}(\text{CO})_4^+$  fragment<sup>11</sup> interacting with either the “saturated”  $\text{C}_3\text{H}_5\text{O}^-$  or the “unsaturated”  $\text{C}_3\text{H}_3\text{O}^-$  fragments. Analysis of the  $\sigma$ -framework of the manganacycles revealed that the HOMO of  $\text{C}_3\text{H}_5\text{O}^-$  and  $\text{C}_3\text{H}_3\text{O}^-$  was centered on the carbon  $\alpha$  to the manganese and that each fragment interacted strongly with  $\text{Mn}(\text{CO})_4^+$  to form a manganese–carbon  $\sigma$ -bond. In addition, manganese complexes **2** and **3** are both stabilized by formation of a  $\sigma$ -bond between the oxygen lone pair of the acyl functional group and the metal. The magnitude of the stabilization afforded to complexes **2** and **3** by dative  $\sigma$ -bond formation is evident from the reactivity of the manganacycles. Nucleophilic donor ligands such as phosphines and phosphites are unable to replace the carbonyl oxygen from the ligand sphere of the metal. For example, manganacycle **11** was unaffected by treatment with triphenylphosphine at room temperature; under more forcing conditions, the reaction of **11** with trimethyl phosphite afforded manganacycle **12** arising from the loss of carbon monoxide rather than cleavage of the

dative manganese–acyl oxygen bond.<sup>1f</sup> Analogously, manganacycle **13** reacts with triphenylphosphine to yield manganacycle **14** rather than phosphine adduct **15**.



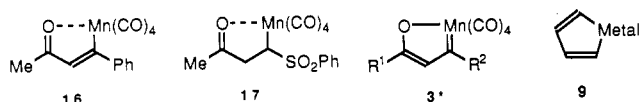
Interestingly, the Mn–O bond distance in manganacycle **16** is nearly identical with that in manganacycle **17**.<sup>10</sup> Nonetheless, the Mulliken populations for the orbitals of the  $\text{C}_3\text{H}_5\text{O}^-$  and  $\text{C}_3\text{H}_3\text{O}^-$  fragments in complexes **2** and **3** indicate that the “unsaturated”  $\text{C}_3\text{H}_3\text{O}^-$  fragment should form a stronger manganese–oxygen bond than the “saturated”  $\text{C}_3\text{H}_5\text{O}^-$  counterpart by virtue of greater donation (0.20e vs 0.14e) to the metal. Moreover, examination of the total overlap populations for the respective

(9) Hall, M. B.; Fenske, R. F. *Inorg. Chem.* 1972, 11, 768.

(10) Geometries for Fenske–Hall calculations of manganacycles **2** and **3** were idealized from the results of X-ray crystallographic studies reported in the supplementary material of ref 1f. The bond angles and lengths of manganacycles **16** and **17** are summarized in Tables III–VI.

(11) Elian, M.; Hoffmann, R. *J. Am. Chem. Soc.* 1975, 97, 4884.

Mn–O interactions reveals that the “unsaturated” complexes of type 3 with a total Mn–O overlap population 0.21e exhibits more covalency than the “saturated” type 2 complexes with a total Mn–O population of 0.18e. Phenomenologically, one might expect that the dative bond in manganacycle 2 would be more readily displaced than in manganacycle 3; however, this was not observed. Neither manganese complex 2 nor 3 displayed a proclivity for displacement of the acyl moiety in the presence of strong donor ligands (*vide supra*). There is also substantial (0.24e) donation from the  $\text{Mn}(\text{CO})_4^+$  fragment into the empty  $3a''$  p orbital of  $\text{C}_3\text{H}_3\text{O}^-$  in 3. This lends credence to the hypothesis that there is a significant contribution of the metallafuran resonance form (i.e. 3\*) in manganacycle 3 which includes a covalent Mn–O bond. The  $1\pi$  and  $2\pi$  orbitals of the unsaturated  $\text{C}_3\text{H}_3\text{O}^-$  fragment do not interact with the metal fragment to any great extent; the Mulliken populations of these canonical orbitals in complex 3 are 2.00 and 1.99 e, respectively.



Invocation of the metallafuran resonance form 3\* for the “unsaturated” manganacycle is justified structurally by the short manganese–carbon bond distance (2.05 Å) observed in type 3 manganacycles such as manganacycle 16 relative to that in the “saturated” analogue (2.12 Å in 17) and by the near equality of the two carbon–carbon bond lengths in manganacycle 16.<sup>10</sup> In addition, we had reported that manganacycle 7 underwent reaction with bromine to provide manganese complex 8 by a process that was analogous to electrophilic aromatic substitution.<sup>1f</sup> It is apparent that metallacycle 3 contains a significantly delocalized  $\pi$ -system and is behaving (by some criteria) as an aromatic compound. This is in contrast to  $d^6$  metallacyclopentadiene complexes 9, such as  $(\eta^5\text{-C}_5\text{H}_5)\text{M}(\text{PR}_3)_2\text{C}_4\text{H}_4$  (M = Co, Rh; R =  $\text{C}_6\text{H}_5$ ,  $\text{C}_6\text{F}_5$ ),<sup>12,13</sup> which show localized C–C single and double bonds. Thorn and Hoffmann<sup>3b</sup> have used MO theory to analyze the bonding in the metallacyclopentadienes and have established sound justification for the lack of delocalization in octahedral  $d^6$  systems. Why, then, is delocalization possible in these manganese complexes? The presence of a highly electronegative heteroatom in the metallacycle severely perturbs the  $\pi$ -system of the organic fragment. The filled  $2\pi$ -orbital of  $\text{C}_3\text{H}_3\text{O}^-$  is disproportionately localized on the oxygen atom with only a negligible contribution from its adjacent carbon atom. As a result, this  $2\pi$ -orbital is nonbonding for the two carbon atoms  $\beta$  to the metal center, whereas the analogous  $2\pi$ -orbital for the metallacyclopentadienes is antibonding between the two  $\beta$ -carbon atoms. This is manifested in a considerable stabilization of the  $2\pi$ -orbital of the  $\text{C}_3\text{H}_3\text{O}^-$  fragment prior to coordination with the metal center. This interaction is favorable inasmuch as there are no low-lying empty orbitals in  $\text{Mn}(\text{CO})_4^+$  that are able to accept charge from  $2\pi$ . Thus the presence of the oxygen atom on the organic fragment obviates Thorn and Hoffmann’s requirement for such an acceptor orbital in order to achieve delocalization.

The empty  $3\pi$ -orbital of  $\text{C}_3\text{H}_3\text{O}^-$  acts as a better acceptor of charge from the metal than does the corresponding orbital of  $\text{C}_4\text{H}_4^{2-}$ . This is again due to the oxygen atom, for its presence lowers the energy of this orbital relative

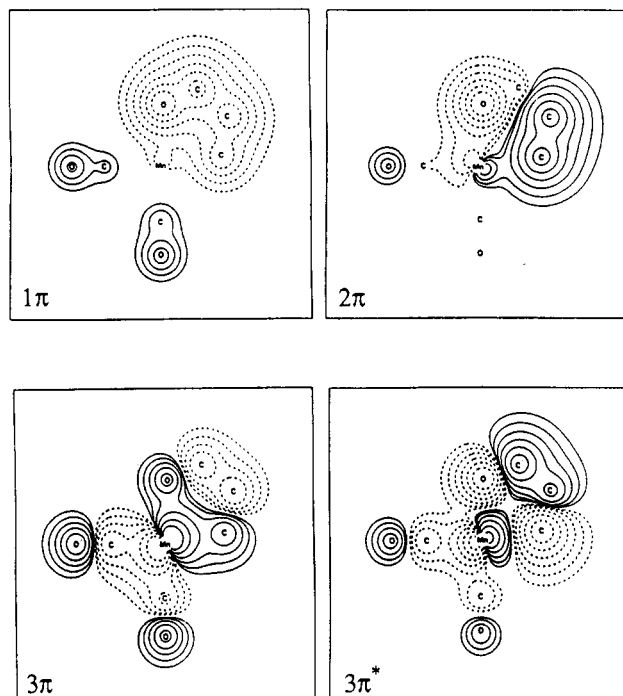


Figure 2. Contour plots of the  $\pi$ -orbitals of manganacycle 3 at 0.20 Å above the plane of the metallacycle. The contour values are 0.005, 0.010, 0.020, 0.040, 0.080, and 0.160.

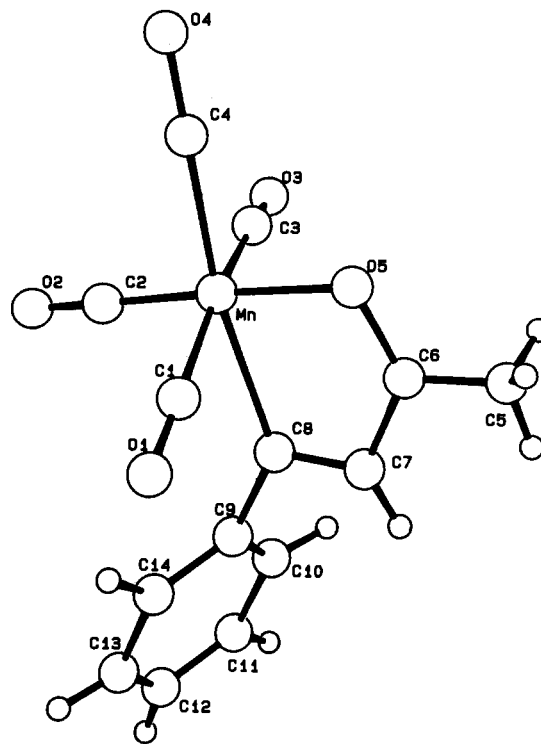


Figure 3. X-ray structure of manganacycle 16. The data are taken from the supplementary material of ref 1f.

to the all-carbon fragment. The back-donation into this orbital (0.24e), while not large, is significantly greater than that observed by Thorn and Hoffmann in the metallacyclopentadienes<sup>3b</sup> and is apparently great enough to impart significant double-bond character to the C–C(O) bond.

Figure 2 shows contour plots of the  $\pi$ -orbitals of manganacycle 3. It is observed that significant Mn atom contributions are found only for the bonding and antibonding interactions between  $3\pi$  and the metal fragment because, as noted above, the  $1\pi$ - and  $2\pi$ - orbitals of the organic moiety are essentially unperturbed by the Mn-

(12) Allen, S. R.; Green, M.; Norman, N. C.; Paddick, K. E.; Orpen, A. G. *J. Chem. Soc., Dalton Trans.* 1983, 1625.

(13) Gastinger, R. D.; Rausch, M. D.; Sullivan, D. A.; Palenik, G. A. *J. Am. Chem. Soc.* 1976, 98, 719; *J. Organomet. Chem.* 1976, 117, 355.

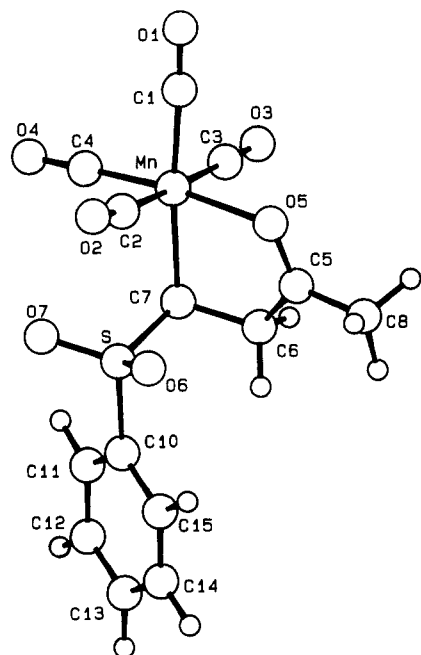


Figure 4. X-ray structure of manganacycle 17.

Table II. Mulliken 3d Electron Populations for Complexes 1-3<sup>a</sup>

	$d_{z^2}$	$d_{x^2-y^2}$	$d_{xy}$	$d_{xz}$	$d_{yz}$	av
MeMn(CO) <sub>5</sub> (1)	0.95	0.92	1.33	1.33	1.14	1.14
C <sub>3</sub> H <sub>5</sub> OMn(CO) <sub>4</sub> (2)	0.89	0.75	1.42	1.33	1.29	1.14
C <sub>3</sub> H <sub>3</sub> OMn(CO) <sub>4</sub> (3)	0.91	0.77	1.45	1.20	1.31	1.13

<sup>a</sup> For complex 1 the methyl carbon is located on the *x* axis, while for complexes 2 and 3 the ring carbon and oxygen atoms lie approximately on the *x* and *y* axes, respectively.

(CO)<sub>4</sub><sup>+</sup> fragment. This is somewhat suggestive of the metallacyclopentatriene MO description proposed by Curtis and Real for a heteroatom-containing nonplanar tantalacycle.<sup>14</sup>

To assess the electronic differences between type 1 complexes and manganacycle complexes 2 and 3, a Fenske-Hall MO calculation was performed upon the type 1 complex MeMn(CO)<sub>5</sub>. The Mulliken 3d atomic orbital populations for complexes 1-3 appear in Table II. Examination of the average 3d orbital populations reveals that the net 3d electron density is consistent with all of the complexes being formally Mn(I) and suggesting that the paramagnetic shift observed does not result from a nephelauxetic effect. Therefore, deformations in the angular distribution of the valence electron density about the nucleus must be principally responsible for the observed deshielding. As can be seen in Table II, there are significant changes in the distribution of electrons between the  $d\sigma$ - and  $d\pi$ -orbitals. First, there is a substantial decrease in the  $3d_{x^2-y^2}$  population for type 1 complexes relative to manganacycles 2 and 3, which corresponds to changes in the  $\sigma$ -bonding of the complexes. Utilizing the Nakatsuji formalism,<sup>6b</sup> we attribute the  $\sigma$ -portion of the paramagnetic shift to the increased hardness of the ketonic oxygen atom relative to carbon monoxide or phosphine ligands. Examination of the  $d\pi$ -orbital populations indicates that there should also be a  $\pi$ -contribution to the paramagnetic shift. The increase in the population of the  $3d_{xy}$  orbital, which lies in the metallacycle plane of complexes 2 and 3, is a consequence of the loss of the in-plane carbon monoxide  $\pi$ -acceptor orbital. This observation is also consistent with

Table III. Bond Lengths (Å) for Manganacycle 16

Mn-O5	2.053	Mn-C1	1.847
Mn-C2	1.798	Mn-C3	1.855
Mn-C4	1.839	Mn-C8	2.040
O1-C1	1.132	O2-C2	1.145
O3-C3	1.131	O4-C4	1.145
O5-C6	1.251	C5-C6	1.493
C6-C7	1.410	C7-C8	1.360

Table IV. Bond Angles (deg) for Manganacycle 16

O5-Mn-C1	92.3	O5-Mn-C2	177.6
O5-Mn-C3	90.3	O5-Mn-C4	94.9
C1-Mn-C2	88.0	C1-Mn-C3	168.4
C1-Mn-C4	94.9	C2-Mn-C3	88.9
C2-Mn-C4	93.2	C3-Mn-C4	96.4
O5-Mn-C8	79.2	C1-Mn-C8	86.4
C2-Mn-C8	98.4	C3-Mn-C8	83.0
C4-Mn-C8	168.4	Mn-O5-C6	114.4
Mn-C1-O1	174.3	Mn-C2-O2	179.3
Mn-C3-O3	173.8	Mn-C4-O4	179.2
O5-C6-C5	119.5	O5-C6-C7	118.2
C5-C6-C7	122.2	C6-C7-C8	116.4
Mn-C8-C7	111.6	Mn-C8-C9	128.4

Table V. Bond Lengths (Å) for Manganacycle 17

Mn-O5	2.055	Mn-C1	18.16
Mn-C2	1.902	Mn-C3	1.848
Mn-C4	1.790	Mn-C7	2.117
S-O6	1.440	S-O7	1.439
S-C7	1.746	S-C10	1.779
O1-C1	1.145	O2-C2	1.086
O3-C3	1.156	O4-C4	1.136
O5-C5	1.242	C5-C6	1.486
C5-C8	1.458	C6-C7	1.517

Table VI. Bond Angles (deg) for Manganacycle 17

O5-Mn-C1	95.3	O5-Mn-C2	87.2
O5-Mn-C3	91.5	O5-Mn-C4	173.5
O5-Mn-C7	79.9	C1-Mn-C2	87.8
C1-Mn-C3	89.5	C1-Mn-C4	90.8
C1-Mn-C7	173.8	C2-Mn-C3	176.8
C2-Mn-C4	90.9	C2-Mn-C7	95.9
C3-Mn-C4	90.9	C3-Mn-C7	86.7
C4-Mn-C7	94.2	Mn-O5-C5	116.7
Mn-C1-O1	176.8	Mn-C2-O2	172.7
Mn-C3-O3	178.7	Mn-C4-O4	179.5
O5-C5-C6	119.3	O5-C5-C8	120.5
C5-C6-C8	110.0	Mn-C7-C6	107.1

Nakatsuji's proposal of increasing paramagnetic shift with increasing  $\pi$ -donation.<sup>6b</sup> Evaluation of the differences in *d* orbital electron populations for complexes 2 and 3 indicates that there is a slight difference in the  $\sigma$ -interactions, as discussed previously; however, it is evident that the major difference involves the  $3d_{xz}$  orbital, which is involved in the  $\pi$ -bonding with the  $\alpha$ -carbon of the manganacycles. As before, increasing  $\pi$ -donation leads to the observed paramagnetic shift for saturated manganacycles 2 relative to 3. It is interesting to note that previous reports have correlated the paramagnetic shift with electronic excitation energies.<sup>6a,d</sup> In this instance, however, the HOMO-LUMO gap for manganacycle 2 is calculated to be 4.08 eV while that of manganacycle 3 is calculated at 3.51 eV. Given the inverse relationship of excitation energy with paramagnetic shift, the observed chemical shifts for complexes 2 and 3 do not correlate with HOMO-LUMO gap.

### Conclusion

In conclusion, it has been demonstrated that <sup>55</sup>Mn nuclear magnetic resonance spectroscopy can be utilized to probe the chemistry of families of Mn(I) complexes. There is a correlation between the chemical shift observed for the metal and the reactivity of manganese complexes 1-3. Molecular orbital calculations support the hypothesis that

(14) Curtis, M. D.; Real, J. *J. Am. Chem. Soc.* 1986, 108, 4668.

the differences in chemical shift observed in the respective families of complexes results from differential donation of electron density from the metal into the organic fragment in the complexes. The calculations also suggest that "unsaturated" manganacycles **3** are aromatic. X-ray data and chemical reactivity studies of **3** also support the hypothesis of aromaticity.

### Experimental Section

**General Information.** Melting points were taken in Kimax soft-glass capillary tubes using a Thomas-Hoover Uni-Melt capillary melting point apparatus (Model 6406 K) equipped with a calibrated thermometer.

Magnetic resonance ( $^1\text{H}$  and  $^{13}\text{C}$  NMR) spectra were recorded on Varian Associates analytical NMR spectrometer (Model EM-360) or a Bruker WP-200, IBM AF-200, or IBM AM-400 spectrometer. Chemical shifts are reported in parts per million ( $\delta$ ) downfield from tetramethylsilane. Coupling constants ( $J$  values) are given in hertz (Hz), and spin multiplicities are indicated by the following symbols: s (singlet), d (doublet), t (triplet), q (quartet), m (multiplet). Deuterated NMR solvents contained 99.0–99.8% deuterium in the indicated position.

Manganese-55 nuclear magnetic resonance spectroscopy was performed at 98.6 or 49.3 MHz on either a IBM AM-400 or a Varian XL-200 spectrometer, respectively. Unless otherwise noted, the spectra were obtained as ca. 0.2 M solutions in benzene- $d_6$  at 298 K. Chemical shift,  $\delta(\text{Mn})$ , values ( $\pm 10$  ppm) are relative to a saturated aqueous solution of  $\text{KMnO}_4$  as an external reference or  $\text{Mn}_2(\text{CO})_{10}$  ( $\delta = 2287$ ) as an internal reference. The width at half-height ( $w_{1/2}$ ) of the  $^{55}\text{Mn}$  signal is reported in kilohertz (kHz).

Infrared spectra were recorded on a Perkin-Elmer Model 281 diffraction grating spectrophotometer or a Nicolet 5DXC Fourier Transform infrared spectrophotometer. Band positions are given in reciprocal centimeters ( $\text{cm}^{-1}$ ) and are listed as br (broad), vs (very strong), s (strong), m (medium), or w (weak).

Mass spectral data were obtained on a Kratos MS-950 double-focusing high-resolution spectrometer, a VG 7070E spectrometer, or on a Finnigan 3200 twin EI and CI quadrupole mass spectrometer equipped with a Finnigan 6000 computer. The chemical ionization gas was methane unless specified otherwise. Elemental analyses were performed by Micro-Tech laboratories, Skokie, IL, or by Dr. F. Kasler of the University of Maryland.

Thin-layer chromatography (TLC) was performed on 0.25-mm Merck silica-coated glass plates, with the compounds being identified in one or more of the following manners: UV (254 nm, unless otherwise specified), iodine, sulfuric acid, or vanillin/sulfuric acid charring. Flash chromatography was performed by using thick-walled glass columns and "medium-pressure" silica (Merck, 32–63  $\mu\text{m}$ ) according to the method of Still.<sup>15</sup> Radial chromatography was performed on a chromatotron (Harrison Research Inc., Palo Alto, CA).

All solvents were distilled from calcium chloride before use unless noted otherwise. Tetrahydrofuran (THF), diethyl ether, benzene, and pentane were distilled from sodium/benzophenone ketyl while triethylamine, pyridine, acetonitrile, and methylene chloride were distilled from calcium hydride. All reagents were distilled, recrystallized, or chromatographed prior to use unless otherwise noted.

Glassware used in the reactions described below was dried in an oven at 120 °C and assembled under an inert atmosphere of nitrogen or argon.

High-pressure reactions were conducted in disposable plastic tuberculin syringes sealed with a luer lock cap. Reaction mixtures were pressurized in a high-pressure apparatus as previously described.<sup>16</sup>

Methylmanganese pentacarbonyl,<sup>17</sup> benzylmanganese pentacarbonyl,<sup>18</sup> *cis*-benzylmanganese tetracarbonyl triphenylphosphine,<sup>18</sup> ( $\eta^1$ -allyl)manganese pentacarbonyl,<sup>19</sup> and phenyl-

manganese pentacarbonyl<sup>20</sup> were prepared according to published procedures.

**Fenske-Hall Molecular Orbital Calculations.** Molecular orbital calculations were undertaken on an IBM 3081-D computer system utilizing the Fenske-Hall nonempirical approximate MO method.<sup>9</sup> In calculations upon  $\text{Mn}(\text{CO})_4\text{C}_3\text{H}_3\text{O}$  and  $\text{Mn}(\text{CO})_4\text{C}_3\text{H}_5\text{O}$  the molecular geometries were based upon the crystal structures of  $\text{Mn}(\text{CO})_4\text{CPhCHCMeO}^{1f}$  and  $\text{Mn}(\text{CO})_4\text{CH}(\text{SO}_2\text{Ph})\text{CH}_2\text{CMeO}^{1f}$ , respectively. Both structures were idealized to  $C_2$  symmetry, which constrains the metallacycles to planarity. In addition, the structural parameters for the  $\text{Mn}(\text{CO})_4$  fragment remain constant for all calculations. In the calculation of  $\text{MeMn}(\text{CO})_5$  the Mn–C(Me) bond distance was taken as 2.19 Å and the Mn–C(CO) bond distance was 1.84 Å. The C–O distances were all set at 1.14 Å, and the symmetry about the metal was locally  $C_{4v}$ .

All atomic wave functions were generated by the method of Bursten, Jensen, and Fenske.<sup>21</sup> Contracted double- $\zeta$  representations were used for the Mn 3d AO's and the C and O 2p AO's. The hydrogen 1s AO utilized an exponent of 1.16.<sup>22</sup> The basis functions for Mn were derived from the +1 oxidation state with fixed 4s and 4p exponents of 2.0 and 1.8, respectively. The carbonyl 3s and 6s orbitals were deleted from the basis transformation set of all calculations.<sup>23</sup> All calculations were performed by using a fragment analysis that has been detailed above.

***cis*-(Phenylacetyl)manganese Tetracarbonyl Tributylphosphine.** To a solution of benzylmanganese pentacarbonyl (250 mg, 0.87 mmol) in THF (10 mL) under  $\text{N}_2$  was added tributylphosphine (240  $\mu\text{L}$ , 0.97 mmol). The solution was stirred in the dark at room temperature for 12 h and then concentrated in vacuo. Purification by flash column chromatography afforded *cis*-(phenylacetyl)manganese tetracarbonyl tributylphosphine (351 mg, 83%) as a pale yellow liquid:  $R_f = 0.43$ ; 9:1 hexanes/ $\text{EtOAc}$ ; IR ( $\text{CCl}_4$ ,  $\text{cm}^{-1}$ ) 3090 (w), 3065 (w), 3030 (w), 2962 (m), 2933 (m), 2875 (m), 2060 (s), 1986 (s), 1962 (s), 1947 (s), 1615 (m), 1465 (w), 1445 (w);  $^1\text{H}$  NMR ( $\text{CDCl}_3$ )  $\delta$  7.15 (m, 5 H), 4.21 (s, 2 H), 1.75 (m, 6 H), 1.37 (m, 12 H), 0.91 (m, 9 H);  $^{13}\text{C}$  NMR ( $\text{CDCl}_3$ )  $\delta$  135.5, 129.7, 128.1, 126.1, 71.7, 26.2 (d,  $J_{\text{P,C}} = 23.5$  Hz), 25.3, 24.2 (d,  $J_{\text{P,C}} = 12.5$  Hz), 13.5; mass spectrum,  $m/z$  (relative intensity, %) 369 (15), 348 ( $\text{M}^+ - 5\text{CO}$ , 34), 285 (17), 257 (100), 91 (35); high-resolution mass spectrum,  $m/z$  348.1786 ( $\text{M}^+ - 5\text{CO}$ , calcd for  $\text{C}_{19}\text{H}_{34}\text{PMn}$ ,  $m/z$  348.1779).

***cis*-Benzylmanganese Tetracarbonyl Tributylphosphine.** *cis*-(Phenylacetyl)manganese tetracarbonyl tributylphosphine (178 mg, 0.36 mmol) was heated at 45–55 °C for 2 h at 0.4 mmHg. Flash column chromatography afforded *cis*-benzylmanganese tetracarbonyl tributylphosphine (62 mg, 74% based on recovered starting material) as a colorless liquid:  $R_f = 0.56$ ; 9:1 hexanes/ $\text{Et}_2\text{O}$ ; IR ( $\text{CCl}_4$ ,  $\text{cm}^{-1}$ ) 2962 (m), 2934 (m), 2875 (w), 2051 (s), 1984 (s), 1958 (s), 1933 (s);  $^1\text{H}$  NMR ( $\text{CDCl}_3$ )  $\delta$  7.46 (br s, 4 H), 7.22 (br s, 1 H), 2.32 (br s, 2 H), 2.08 (br s, 6 H), 1.79 (br s, 12 H), 1.30 (br s, 9 H);  $^{13}\text{C}$  NMR ( $\text{CDCl}_3$ )  $\delta$  154.2, 128.1, 125.6, 122.1, 26.2 (d,  $J_{\text{P,C}} = 2.0$  Hz), 25.3, 24.3 (d,  $J_{\text{P,C}} = 12.5$  Hz), 13.5, 12.0 (d,  $J_{\text{P,C}} = 9.5$  Hz); mass spectrum,  $m/z$  (relative intensity, %) 369 (4), 348 ( $\text{M}^+ - 4\text{CO}$ , 8), 257 (43), 91 (100); high-resolution mass spectrum,  $m/z$  348.1775 ( $\text{M}^+ - 4\text{CO}$ , calcd for  $\text{C}_{19}\text{H}_{34}\text{PMn}$ ,  $m/z$  348.1779).

***cis*-Methylmanganese Tetracarbonyl Tributylphosphine and *cis*-Acetylmanganese Tetracarbonyl Tributylphosphine.** Tributylphosphine (325  $\mu\text{L}$ , 1.31 mmol) was added to a solution of methylmanganese pentacarbonyl (250 mg, 1.19 mmol) in THF (10 mL). The mixture was stirred in the dark at room temperature under  $\text{N}_2$  for 12 h. Concentration in vacuo and purification by flash column chromatography afforded *cis*-methylmanganese tetracarbonyl tributylphosphine (112 mg) as a pale yellow liquid and *cis*-acetylmanganese tetracarbonyl tributylphosphine (323 mg) as a colorless liquid (90% overall yield).

(19) McClellan, W. R.; Hoehn, H. H.; Cripps, H. N.; Muettterties, E. L.; Howk, B. W. *J. Am. Chem. Soc.* 1961, 83, 1601.

(20) Coffield, T. H.; Kozikowski, J.; Clossen, R. D. *J. Org. Chem.* 1957, 22, 598.

(21) Bursten, B. E.; Jensen, J. R.; Fenske, R. F. *J. Chem. Phys.* 1978, 68, 3320.

(22) Herhe, W. J.; Stewart, R. F.; Pople, J. A. *J. Chem. Phys.* 1969, 51, 2657.

(23) Lichtenburger, D. L.; Fenske, R. F. *J. Chem. Phys.* 1976, 64, 4247.

(15) Mitra, A.; Kohn, M.; Still, W. C. *J. Org. Chem.* 1978, 43, 2923.

(16) DeShong, P.; Dicken, C. M.; Perez, J. J.; Shoff, R. N. *Org. Prep. Proced. Int.* 1983, 14, 369.

(17) Clossen, R. D.; Kozikowski, J.; Coffield, T. H. *J. Org. Chem.* 1957, 22, 598.

(18) Drew, D.; Darensbourg, M. Y.; Darensbourg, D. J. *J. Organomet. Chem.* 1975, 85, 73.

*cis*-Methylmanganese tetracarbonyl tributylphosphine:  $R_f = 0.65$ ; 9:1 hexanes/Et<sub>2</sub>O; IR (CCl<sub>4</sub>, cm<sup>-1</sup>) 2962 (m), 2934 (m), 2875 (m), 2053 (s), 1977 (s), 1959 (s), 1930 (s); <sup>1</sup>H NMR (CDCl<sub>3</sub>) δ 1.69 (br s, 6 H), 1.43 (br s, 12 H), 0.94 (br s, 9 H), -0.47 (br s, 3 H); <sup>13</sup>C NMR (CDCl<sub>3</sub>) δ 26.2 (d,  $J_{P,C} = 23.0$  Hz), 25.2, 24.2 (d,  $J_{P,C} = 12.5$  Hz), 13.5, -17.3 (d,  $J_{P,C} = 10.0$  Hz); mass spectrum,  $m/z$  (relative intensity, %) 384 (2), 300 (17), 272 (M<sup>+</sup> - 4CO, 100), 257 (38); high-resolution mass spectrum,  $m/z$  272.1465 (M<sup>+</sup> - 4CO, calcd for C<sub>13</sub>H<sub>30</sub>PMn,  $m/z$  272.1466). *cis*-Acetylmanganese tetracarbonyl tributylphosphine:  $R_f = 0.31$ ; 9:1 hexanes/Et<sub>2</sub>O; IR (CCl<sub>4</sub>, cm<sup>-1</sup>) 2962 (m), 2933 (m), 2875 (m), 2060 (m), 1986 (s), 1961 (s), 1947 (s), 1634 (m); <sup>1</sup>H NMR (CDCl<sub>3</sub>) δ 2.53 (br s, 3 H), 1.76 (br s, 6 H), 1.38 (br s, 12 H), 0.92 (br s, 9 H); <sup>13</sup>C NMR (CDCl<sub>3</sub>) δ 52.1, 26.2 (d,  $J_{P,C} = 24.0$  Hz), 25.2, 24.2 (d,  $J_{P,C} = 12.5$  Hz), 13.5; mass spectrum,  $m/z$  (relative intensity, %) 384 (3), 369 (1), 300 (19), 272 (M<sup>+</sup> - 5CO, 100), 257 (39); high-resolution mass spectrum,  $m/z$  272.1478 (M<sup>+</sup> - 5CO, calcd for C<sub>13</sub>H<sub>30</sub>PMn,  $m/z$  272.1466).

**Bromination of Manganacycle 7: Formation of Manganacycle 8.** Bromination of manganacycle 7 has been described previously.<sup>1f</sup>

**Manganacycle 12.** The preparation of manganacycle 12 has been previously described.<sup>1f</sup>

**Reaction of Manganacycle 13 and Triphenylphosphine.** A hexane (4 mL) solution of manganacycle 13 (72 mg, 0.19 mmol) and triphenylphosphine (76 mg, 0.29 mmol) was stirred at room temperature in the dark for 21 h. Evaporation of the solvent and chromatography of the residue on silica gave 94 mg (82%) of manganacycle 14 as a pale yellow gum. The product was a single

diastereomer as determined from the <sup>31</sup>P NMR spectrum and was assigned the *fac* stereochemistry based upon the CO pattern in the infrared spectrum:  $R_f = 0.13$ ; 4:1 hexane/EtOAc; IR (CCl<sub>4</sub>, cm<sup>-1</sup>) 2017 (s), 1940 (s), 1906 (s), 1678 (m), 1641 (w), 1436 (m), 1163 (m); <sup>1</sup>H NMR (C<sub>6</sub>D<sub>6</sub>, very broad signals) δ 7.78, 7.23, 4.02, 3.58, 2.89; <sup>13</sup>C NMR (C<sub>6</sub>D<sub>6</sub>) δ 232.5, 183.8, 134-128, 50.3, 48.5, 47.1, 31.6 (d,  $J_{P,C} = 10.0$  Hz); <sup>31</sup>P NMR (C<sub>6</sub>D<sub>6</sub>, vs H<sub>3</sub>PO<sub>4</sub>) δ 56.3 (s).

**Preparation of Type 2 and Type 3 Manganese Complexes.** The preparation of type 2 and type 3 adducts of methyl- and benzylmanganese pentacarbonyl has been described previously.<sup>1f</sup>

**Acknowledgment.** Generous financial support from the Public Health Service, National Institute of Health (P.D.; GM 37014 and AI 23688) and the Swiss National Science Foundation (W.v.P.; 2.033.086) is gratefully acknowledged. B.E.B. is a Camille and Henry Dreyfus Foundation Teacher-Scholar (1984-1989). Numerous helpful discussions with Professor Rinaldo Poli (University of Maryland) are acknowledged.

**Registry No.** 1 (R = Me), 13601-24-6; 3 (R<sup>3</sup> = Me), 25281-94-1; 3 (R<sup>3</sup> = PhCH<sub>2</sub>), 113749-00-1; 6, 113748-89-3; 7, 113749-01-2; 8, 113749-02-3; 10, 54834-89-8; 11, 88996-56-9; 12, 88996-58-1; 13, 113748-96-2; 14, 120311-01-5; η<sup>1</sup>-H<sub>2</sub>C=CHCH<sub>2</sub>Mn(CO)<sub>5</sub>, 14057-83-1; PhCH<sub>2</sub>Mn(CO)<sub>4</sub>(PBU<sub>3</sub>), 120408-29-9; PhCH<sub>2</sub>Mn(CO)<sub>5</sub>, 14049-86-6; PhMn(CO)<sub>5</sub>, 13985-77-8; CH<sub>3</sub>C(O)Mn(CO)<sub>4</sub>(PBU<sub>3</sub>), 105180-21-0; PhCH<sub>2</sub>C(O)Mn(CO)<sub>4</sub>(PBU<sub>3</sub>), 120311-00-4; *cis*-methylmanganese tetracarbonyl tributylphosphine, 105180-19-6.

## Organometallic Compounds of the Lanthanides. 48.<sup>1</sup> Cyclooctatetraenyl Pentamethylcyclopentadienyl Derivatives of the Rare Earths

Herbert Schumann,\* Randolf D. Köhn, Friedrich-Wilhelm Reier, Andreas Dietrich, and  
Joachim Pickardt

Institut für Anorganische und Analytische Chemie der Technischen Universität Berlin,  
D-1000 Berlin 12, Bundesrepublik Deutschland

Received March 23, 1988

The reaction of (C<sub>8</sub>H<sub>8</sub>)LnCl(THF)<sub>n</sub> compounds (Ln = Pr, Sm, Gd, Tb, Dy, Er, and Lu) with NaC<sub>5</sub>Me<sub>5</sub> in tetrahydrofuran leads to cyclooctatetraenyl pentamethylcyclopentadienyl rare earth complexes of the type (C<sub>8</sub>H<sub>8</sub>)Ln(C<sub>5</sub>Me<sub>5</sub>)(THF)<sub>x</sub> (2). These compounds were characterized by elemental analyses and NMR and mass spectroscopy. The X-ray structural analysis of (C<sub>8</sub>H<sub>8</sub>)Lu(C<sub>5</sub>Me<sub>5</sub>) (2i) shows it to be orthorhombic with  $a = 10.282$  (2),  $b = 11.549$  (2), and  $c = 12.969$  (2) Å, space group *Pnam*,  $Z = 4$ , and  $D(\text{calcd}) = 1.787$  g cm<sup>-3</sup>. The structure was solved from 1766 observed reflections with  $F_o \geq 3\sigma(F_o)$  and refined to a final *R* factor of 0.024. The expected sandwich molecular structure is only slightly bent according to the ring centroid-Lu-ring centroid angle of 173°.

### Introduction

Mixed-sandwich compounds of the type (C<sub>8</sub>H<sub>8</sub>)M(C<sub>5</sub>H<sub>5</sub>) have been known since 1969 when Oven and Liefde Meijer<sup>2</sup> prepared (C<sub>8</sub>H<sub>8</sub>)Ti(C<sub>5</sub>H<sub>5</sub>). The crystal structure of this complex was solved 1 year later by Kroon and Helmholdt.<sup>3</sup> Soon after, analogous compounds of the group 3 elements Sc<sup>4</sup> and Y<sup>5</sup> as well as of the lanthanides Nd, Sm, Ho, and Er<sup>5</sup> were prepared from (C<sub>8</sub>H<sub>8</sub>)LnCl and NaC<sub>5</sub>H<sub>5</sub> or

C<sub>5</sub>H<sub>5</sub>LnCl<sub>2</sub> and K<sub>2</sub>C<sub>8</sub>H<sub>8</sub>. However, the starting cyclooctatetraenyl rare earth chlorides as well as the mixed sandwiches have not been characterized very well; some of them have been formulated as solvent-free complexes and some as adducts with one or two THF molecules. On the basis of the X-ray structural analyses of (C<sub>8</sub>H<sub>8</sub>)-CeCl(THF)<sub>2</sub><sup>7,8</sup> and (C<sub>8</sub>H<sub>8</sub>)NdCl(THF)<sub>2</sub><sup>9</sup> which show the

(5) Jamerson, J. D.; Masino, A. P.; Takats, J. J. *Organomet. Chem.* 1974, 65, C33.

(6) Hodgson, K. O.; Mares, F.; Starks, D. F.; Streitwieser, A. *J. Am. Chem. Soc.* 1973, 95, 8650.

(7) Mares, F.; Hodgson, K. O.; Streitwieser, A. *J. Organomet. Chem.* 1971, 28, C24.

(8) Hodgson, K. O.; Raymond, K. N. *Inorg. Chem.* 1972, 11, 171.

(9) Shen, Q.; Chen, W.; Jin, Y.; Shan, C. *Pure Appl. Chem.* 1988, 60, 1251.

(1) Part 47: Schumann, H.; Janiak, C.; Köhn, R. D.; Loebel, J.; Dietrich, A. *J. Organomet. Chem.*, in press.

(2) van Oven, H. O.; de Liefde Meijer, H. J. *J. Organomet. Chem.* 1969, 19, 373.

(3) Kroon, P. A.; Helmholdt, R. B. *J. Organomet. Chem.* 1970, 25, 451.

(4) Westerhof, A.; de Liefde Meijer, H. J. *J. Organomet. Chem.* 1976, 116, 319.